

CFD Evaluation of Radiative and Natural Convective Conjugate Heat Transfer in the Gap Space between Small Modular Reactor Vessel and Metal Containment during Normal Operation

Geonhyeong Lee¹, Taeseok Kim¹, and Sung Joong Kim^{1,2}

¹Department of Nuclear Engineering, Hanyang University
222 Wangsimni-ro, Seongdong-gu, Seoul 04763, Republic of Korea

²Institute of Nano Science and Technology, Hanyang University
222 Wangsimni-ro, Seongdong-gu, Seoul 04763, Republic of Korea
ghlee9605@hanyang.ac.kr;tkim@hanyang.ac.kr; sungjkim@hanyang.ac.kr

1. Introduction

According to the IAEA classification, small modular reactors (SMRs) refer to the reactors that produce electrical power lower than 300 MWe [1]. These SMRs have drawn great attention owing to its advantages with improved inherent safety and enhanced co-generation scheme with renewable energy.

Interestingly, many SMRs adopted a distinctive structure called a double-vessel structure which consists of a Reactor Pressure Vessel (RPV) with a surrounding metal containment vessel (MCV), from which an empty or buffer space called a gap naturally forms. This structure is designed to retain radioactive materials escaping from the RPV and enables long-term cooling through external cooling in the event of an accident. In addition, the gap that can be filled with various substances such as inert gas or vacuumized serves as a thermal insulator that improves thermal efficiency during normal operation.

NuScale under development in U.S. is such an example adopting the double-vessel structures. The NuScale insists that vacuumizing the gap can be the best insulator to prevent heat loss through conduction and convection heat transfer. Nonetheless, however, radiative heat transfer cannot be eliminated permanently because the radiative heat transfer can be promoted in the vacuum condition and the normal operating temperature of the SMR is as high as 320 °C (593 °K).

Similarly, an innovative-SMR (i-SMR) under development in Korea also considers the various gap fillers including vacuumed gap for the design. As such, this study investigates heat loss characteristics upon various stagnant gases in the gap with sufficiently low conductivity preventing conductive heat transfer. Filling the gap with the low conductivity gas could be a reasonable strategy due to relatively less maintenance costs than the vacuuming. Because the proposed gas-filled gap conditions generate natural convective and radiative heat transfer, however, a systematic study on the heat loss mechanism should be conducted. Albeit its importance on the heat loss through the gap space, however, any relevant research on natural convective and radiative heat transfer in the gap of the double-vessel structure has not been reported to date.

So the objective of this study is to identify the heat loss mechanism according to the gap filler material and to

quantify the radiative heat insulation effect on the proposed i-SMR during the normal operation. In order to fulfill the aforementioned purpose, computational fluid dynamics (CFD) simulation was performed with ANSYS FLUENT 21.2. To analyze the effect of natural convection, various gases such as air, carbon dioxide, argon, and xenon, including the vacuum conditions, were selected as the gap filler. In addition, the radiative heat effect was also identified separately by using radiative heat insulation with an emissivity of 0.04. Based on the simulation results, an optimal gas filler for the proposed i-SMR was derived as a replacement for vacuum conditions.

2. Methodology of CFD simulation

To confirm the effects of gap filler and radiative heat insulation inside the gap, a comprehensive CFD analysis was conducted. In this section, heat transfer mechanism, mesh generation, and solver settings for CFD simulation were described.

2.1. Heat transfer process in double vessel structure

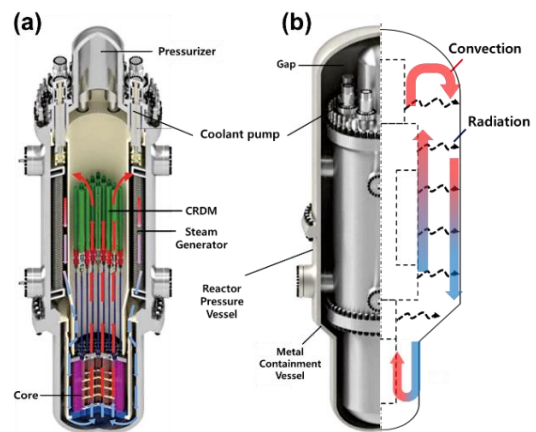


Figure 1. Placement of (a) components inside the RPV (b) and double vessel structure and natural convective flow of the i-SMR.

Fig. 1 (a) shows the placement of NSSS components inside the RPV of the i-SMR. Within the RPV, the core is located at the bottom, the pressurizer is located at the top, and the steam generator is located at the upper region

of the RPV inside. In addition, motor-canned reactor coolant pumps are located above the steam generator. During normal operation, the heated coolant is circulated through the pumps and transfers heat from the core to the steam generator and flows down along the inner wall of the RPV. In this process, unintended heat transfer can occur to the RPV wall.

Fig. 1 (b) shows the geometric characteristics of the double vessel structure of the i-SMR and heat transfer mechanism inside the proposed i-SMR gap. During the normal operation, conduction heat transfer occurs in each vessel. In addition, natural convective and radiative heat transfers are expected to occur inside gap. Therefore, to reduce the heat loss, it is necessary to adjust the thermal and radiation properties.

2.2. Parameters of the natural convective heat transfer

In general, the intensity of the natural convective flow is characterized by the Rayleigh number (Ra) defined by Eq. (1). The higher the Ra number, the higher the heat transfer performance. In other words, the insulation performance can be deemed excellent when the Ra number is low.

$$Ra = PrGr = \frac{\nu g\beta\Delta TL^3}{\alpha \nu^2} = \frac{g\beta\Delta TL^3}{\alpha} \quad (1)$$

For the same geometry, natural convection is affected by thermal properties such as kinematic viscosity (ν), specific heat capacity (c_p), thermal conductivity (k), and density (ρ), as shown in Eq. (1). Accordingly, natural convection performance can be differed depending on the convective media. To investigate this difference, air, argon, carbon dioxide, xenon, and the vacuum conditions were selected as the potential candidates. In this study, vacuum conditions were approximated by adjusting the thermal properties of air under 1 mbar pressure conditions. When the insulation performance is evaluated only through thermal properties, the heat loss is expected to be small in the order of vacuum conditions, xenon, argon, air, and carbon dioxide.

2.3. Parameter of the radiative heat transfer

Heat transfer in the gap occurs not only by natural convective but also by radiative heat transfer. Interestingly, a recent study reports that the heat loss by the radiative heat can be more dominant in gas space [2]. A governing equation of the radiative heat transfer is shown in Eq. (2), which includes a critical surface parameter, viz., emissivity (ϵ). The emissivity is a value that indicates how much radiation is emitted compared to the black body, and its values ranges between 0 and 1.

$$Q_R = \epsilon_{effective} \sigma A (T_{surface}^4 - T_{surrounding}^4) \quad (2)$$

In the same geometry, it is determined that heat loss due to radiative heat transfer may be reduced by reducing the emissivity. Therefore, if the RPV or MCV wall surface is altered to a low emissivity by using a surface treatment technique, the radiative heat transfer can be sufficiently reduced. In this study, it was assumed that the RPV is made of carbon steel (SA508), which is widely used for conventional RPVs. In addition, the MCV was assumed to be made of stainless steel (SS316), which has better corrosion resistance than SA508. The properties of the double vessel materials are specified in Table 1, in which the emissivity of each MCV and RPV was confirmed to be 0.4 and 0.7 [3].

Table 1: Properties of the vessel materials.

	SA508 (RPV)	SS316 (MCV)
ρ (kg/m ³)	7,833	7,870
c_p (J/kg·K)	465	490
k (W/m·K)	54	13
ϵ (-)	0.7	0.4

To insulate the radiative heat effectively, use of materials with low emissivity is advantageous apparently. So it is assumed that the emissivity could be reduced by as much as 0.04 by introducing a thin aluminum foil, which is a highly reflective surface for insulating the radiative heat. Although the emissivity may increase as the aluminum foil is oxidized, a single emissivity value was introduced by assuming no oxidation. To apply this into the CFD simulation, it was assumed that the inner wall of the MCV was treated with special coating to prevent radiative heat. As a result, the emissivity value was lowered from 0.4 to 0.04.

In addition, in the case of carbon dioxide, which is a polar molecule, unlike other gases, has an absorption coefficient that absorbs radiation. Therefore, it can affect the thermal radiation behavior in the gap. In this study, the absorption coefficient of carbon dioxide was set to 0.43 (m⁻¹), which is a default value in the FLUENT library.

2.4. Mesh generation and settings for CFD simulation

Creating an appropriate geometry for areas of interest is an important process in CFD analysis. However, the i-SMR is a reactor under conceptual design stage, so an accurate geometric information is unavailable as of current writing. In this study, therefore, a geometry of the double-vessel structure with an arbitrary size was produced. The size of the shape is shown in Table 2.

Table 2: Size of the vessel components

	SA508 (RPV)	SS316 (MCV)
Height (m)	13.44	14.886
Outer radius (m)	0.84-1.68	2.022-2.273
Thickness (m)	0.13	0.09

Simulating the vessel components suggested in Table 2 in 3D CFD requires very expensive computational costs. For a reasonable calculation time, therefore, the calculation was performed based on a 2D symmetry condition. The tentative i-SMR geometry was produced by using ANSYS Design Modeler 17.0, and the information on the geometry and boundary conditions is shown in Fig. 2.

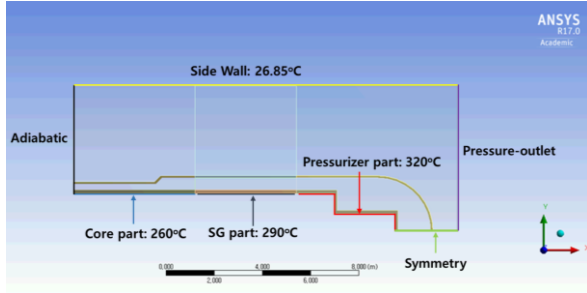


Figure 2. i-SMR 2D geometry and boundary conditions

To reflect the axial coolant temperature distribution during the normal operation, the temperature of the inner wall of the RPV was divided into three parts and set differently to 320 (red line), 290 (gray line), and 260°C (blue line), from top to bottom, respectively. The coolant inlet/outlet temperature was referred from the NuScale design. In addition, the axisymmetric condition (green line) was applied by setting the x-axis as the center line according to the FLUENT manual. Additionally, to assume an open ambient, the upper side of the i-SMR was set to Pressure-outlet (violet line). Finally, the rest of the walls were set as default temperature (yellow line) and adiabatic condition (black line).

To ascertain the reliability of the mesh, mesh sensitivity analysis was conducted. There were four (1,215,983, 1,571,052, 2,135,664, and 3,851,764) meshes produced for the analysis, and the results were compared for the temperature distribution and temperature gradient. Except for the smallest mesh number, however, a difference within 1 % was observed in the results according to mesh size. Therefore, based on the sensitivity analysis, a subsequent CFD calculation was performed with 2,135,664 nodes of medium size.

To conduct the simulation, it is necessary to make reasonable assumptions and to select the relevant solver.

The assumptions adopted in this study are as follows:

- 1) Constant RPV inner wall temperature: During normal operation, the circulating coolant maintains the constant temperature (steady-state).
- 2) Gray radiation: In case of radiation, it exhibits the same emissivity regardless of wavelength.
- 3) Thickness of the aluminum foil is very thin. Therefore, it does not create an additional thermal resistance.
- 4) Boussinesq approximation: In the case of gas density, it changes linearly (Eq. (3)).

$$\rho = \rho_0 - \beta\rho_0(T - T_0) \quad (3)$$

The solver settings were summarized in Table 3. Many studies report that the SST k-omega model is optimized for natural convection near the wall [4]. Therefore, this study also adopted the SST k-omega turbulent model. In addition, radiative heat transfer was calculated by using the Discrete Ordinates (DO) model used widely owing to its moderate computational cost and availability for all optical thickness ranges. In the case of Spatial Discretization, the pressure term was set Body Force Weighted to simulate buoyancy-driven flow. Finally, the Pressure-Velocity Coupling used Coupled because it tended to reduce convergence time by calculating kinetic energy and temperature fields at once.

Table 3: solver and model settings

Turbulent Model	SST k-omega	
Density Model	Boussinesq approximation	
Radiation Model	DO gray Model	
Scheme	Coupled	
Spatial Discretization	Gradient	Least Squares Cell Based
	Pressure	Body Force Weighted
	Momentum	2 nd Order Upwind
	Energy	2 nd Order Upwind

3. Results and discussion

In this study, the calculation was judged sufficiently converged when the residuals were decreased below the set criteria. Each criterion is set for continuity, k, and epsilon was 10^{-3} and the energy was 10^{-6} . In this section, the results of the above-mentioned gap filler and radiative heat transfer insulation effects are described.

3.1. Total heat loss depending on the gap fillers

Although the total heat transfer rate of the inner wall and outer wall of the MCV is equal, the ratio of radiative heat loss to the total heat loss is calculated differently because the temperatures at each wall are different. Thus, this study focused on the heat transfer within the gap and the analysis was conducted on the MCV inner wall. The heat transfer rates [W] on the MCV inner wall without radiative heat (w/o rad.) and with radiative heat ($\epsilon=0.4$) are summarized in Fig. 4.

To compare the natural convective heat transfer performance with the applying gap materials, the simulation case without radiative heat transfer was preferentially performed and set as the reference. If the thermal radiation is not considered, vacuum conditions could be the best among the candidates. This is reasonable because heat transfer occurs weakly only with conduction and natural convection when the thermal radiation is not considered. In cases of the remaining candidates except for the vacuum condition, the insulation performance was excellent in the order of

xenon, argon, air, and carbon dioxide. Xenon and argon showed the similar performance but air and carbon dioxide differed significantly with each other. Particularly carbon dioxide was 42% higher than xenon. These differences were identical to the performance order of natural convection mentioned in Section 2.2 and it can be judged that thermal properties affect the natural convection predominantly.

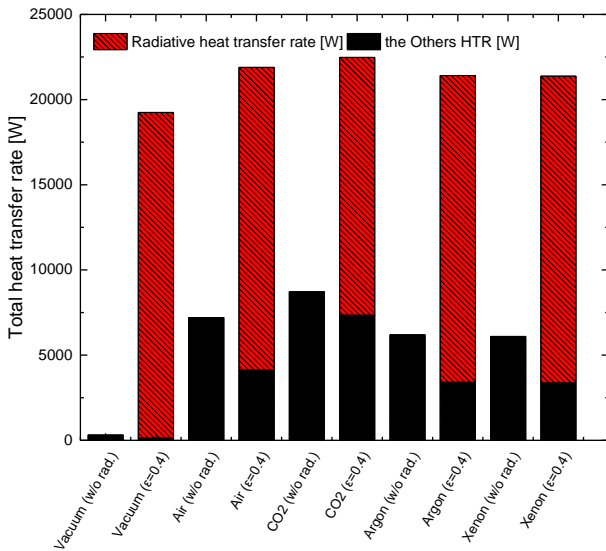


Figure 4. Comparison of radiative heat transfer rate (red and diagonal) and other heat transfer rate (black) depending on the presence of radiation on the MCV wall.

To analyze the effect of the radiation, additional cases considering the radiative heat transfer were performed. It can be noted that when thermal radiation is present, the insulation performance is greatly lowered and the difference between filler gases and vacuum conditions is reduced to 10%. It is because vacuum conditions, where most heat transfer is performed by thermal radiation, facilitate more radiative heat transfer than the rest of the candidate groups. The results indicate that at least in the perspective of the heat loss minimization, the i-SMR does not necessarily have to maintain the vacuum conditions because the difference from the gas is not significant. Furthermore, carbon dioxide is still the worst insulator in the remaining gas candidates, but it can be seen that the difference with xenon has decreased from 42 to 5%. This could be because the less thermal radiation is transferred since carbon dioxide absorbed more heat by setting an absorption coefficient. In addition, as previously confirmed it is because the performance of natural convection is also higher. Although the amount of radiative heat transfer is different in each candidate, it can be confirmed that thermal radiation is the dominant mechanism in all candidate groups. Therefore, if this thermal radiation is reduced through any practical technique, more competitive insulation can be realized.

3.2. The thermal radiation insulation effect on the MCV wall

To confirm the effect of the aforementioned method, this study considered a method of reducing radiative heat transfer rate by coating aluminum foil on the inner wall surface of MCV as arbitrary radiation shielding. The results are summarized in Fig. 5.

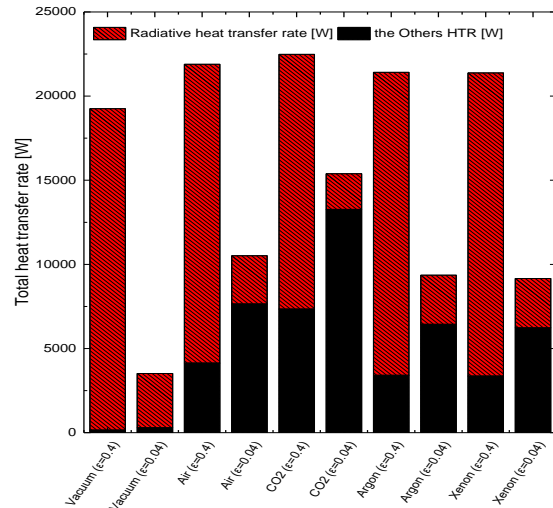


Figure 5. Comparison of heat loss by radiation heat transfer insulation effect. This separates the radiative heat transfer (red and diagonal) and other heat transfer rates (black) on the MCV wall.

The emissivity of MCV was reduced from 0.4 to 0.04 by coating aluminum foil. As a result, the heat loss was reduced by 82% for vacuum, and up to 57% for gases in xenon. On the other hand, in case of carbon dioxide, heat loss due to radiation was greatly reduced but the heat loss due to natural convection increased by approximately 80%, and the total heat loss decreased by only 32%. In summary, conditions showing excellent performance of thermal radiation insulation effect were identified in order of vacuum (reduction rate: 82%), xenon (57%), argon (54%), air (52%), and carbon dioxide (32%).

In addition, the case where thermal radiation insulation was absent under vacuum conditions and the cases with thermal radiation insulation under gas filling conditions were compared. As a result, in case of thermal radiation insulation for the gas filler, the total heat loss was reduced in all cases compared to vacuum conditions without thermal radiation insulation. The reduction rate was evaluated in order of xenon (reduction rate: 52%), argon (51%), air (43%), and carbon dioxide (20%).

From these results, it is suggested that if vacuum conditions and thermal radiation insulation are difficult to apply simultaneously in the gap of i-SMR, applying stagnant pressure xenon and radiation shielding could be a more reasonable strategy in terms of insulation performance.

3. Conclusions

In this paper, a study was conducted on gas filling conditions that can replace vacuum conditions for the proposed i-SMR gap conditions that have not yet been determined. Based on the simulation results performed for thermal radiation insulation effects, the following conclusions can be drawn.

1. The radiative heat transfer was the dominant heat transfer mechanism not only in the gases but also in the vacuum conditions. At this time, the better insulation performance was shown in the order of vacuum conditions, xenon, argon, carbon dioxide, and air.

2. Among the gas fillers, thermal radiation insulation is most effective in xenon (optimal gas filler) and least effective in carbon dioxide.

3. All the gas fillers with thermal radiation insulation exhibit better insulation performance than vacuum conditions without thermal radiation insulation. Therefore, at least in the perspective of heat loss minimization, the stagnant xenon gas with thermal radiation insulation can sufficiently replace the vacuum condition.

This study helps to understand the characteristics of the overall heat loss mechanism and identify the effects of thermal radiation insulation. However, there is a limit to confirming validity because CFD results have not been verified with experimental results. Therefore, the experimental apparatus will be manufactured as soon as possible and the evaluation of thermal radiation insulation effects will be identified.

Acknowledgement

This work was supported by the National Research Foundation of Korea (NRF) grant funded by the Korea government (MSIT) (No. NRF-2022M2D2A1A02061334).

REFERENCES

- [1] F. Reitsma et al., "Advances in Small Modular Reactor Technology Developments," *IAEA Advanced Reactors Information System (ARIS)*, (2020).
- [2] Hangbin Zhao et al., "Numerical simulation on heat transfer process in the reactor cavity of modular high temperature gas-cooled reactor," *Applied Thermal Engineering*, (2017).
- [3] Christian Gaigl et al., "Technical Report, Thermal impact on HDG construction," *Technical University of Munich*, (2018).
- [4] G. Vijaya Kumar et al., "CFD modelling of buoyancy driven flows in enclosures with relevance to nuclear reactor safety," *Nuclear Engineering and Design*, (2020).